https://chemclassjournal.com/
ChemClass Journal Vol. 9 Issue 2 (2025); 672-690
e-ISSN:3092-8214 p-ISSN:3092-8206
doi.org/10.33003/chemclass-2025-0902/189

Green Synthesis and Antimicrobial Activity of *Spondias mombin*-Derived Iron and Copper Nanoparticles Against *Staphylococcus aureus* and *Aspergillus niger*

[1]Eze, Uchenna Samson; [2]* James, Abosede Olubunmi

[1]Department of Chemistry Education, Federal College of Education (Technical) Omoku. Rivers State, Nigeria

** [2]Department of Pure and Industrial Chemistry, University of Port Harcourt, Rivers State, Nigeria*

(*)Corresponding Author's: ezesamson@fcetomoku.edu.ng *Tel: +2349154595519

Co-Authors Email: abosede.james@uniport.edu.ng

Abstract

This study examines the antimicrobial capabilities of iron and copper nanoparticles synthesized using Spondias mombin leaf extract against clinical isolates of Aspergillus niger and Staphylococcus aureus. The iron nanoparticles (Sm-FeNPs) and copper nanoparticles (Sm-CuNPs) were synthesized using a green approach and then characterized using techniques such as UV-Vis spectroscopy, X-Ray Diffraction Analysis (XRD), Scanning Electron Microscopy (SEM), Fourier-transform infrared spectroscopy (FTIR), and Particle Size Analysis (PSA). The nanoparticles were then tested at different (5–30 mg/mL) concentrations using the agar well diffusion method. By measuring the size of the clear zones surrounding the wells, the antimicrobial activity was ascertained. This was followed by the determination of the minimum inhibitory concentration (MIC), which aids in determining the lowest concentration at which microbial growth can be inhibited. From the results obtained, Sm-CuNPs exhibited quantitatively stronger antimicrobial effects than Sm-FeNPs, producing inhibition zones ranging from 6.5–14.0 mm for Staphylococcus aureus and 5.25–12.0 mm for Aspergillus niger, compared to 6.0–11.0 mm and 4.0–9.0 mm respectively for Sm-FeNPs. Sm-CuNPs achieved a MIC of 10 mg/mL for both organisms, whereas Sm-FeNPs achieved a MIC of 10 mg/mL for Staphylococcus aureus and 20 mg/mL for Aspergillus niger. These findings show that Sm-CuNPs were more effective against the two tested microbes. This is attributed to their ability to damage cell membranes and generate reactive oxygen species (ROS) that harm microbial cells. Since Sm-CuNPs showed significant activity against both bacterial and fungal isolates, it suggests their potential usefulness in treating infections caused by Staphylococcus aureus and Aspergillus niger. Moreover, the study highlights the ecological benefit of using Spondias mombin leaf extract for nanoparticle synthesis, supporting the growing interest in eco-friendly nanotechnology for antimicrobial applications.

Keywords : Antimicrobial, *Aspergillus niger,* Green Chemistry, S*pondias mombin*, *Staphylococcus aureus*.

Introduction

Nanotechnology has been in the spotlight due to its wide range of applications from electronics to medicine [1]. In particular, the synthesis and use of metal nanoparticles (NPs) have received much attention lately. This is because they show promising potential in biomedical applications, especially for treating infections [2]. Among these nanoparticles, CuNPs and FeNPs have been widely studied for their antimicrobial properties against bacteria and fungi [3]. According to recent studies, the increasing resistance of microbes towards antibiotics has led many researchers to seek alternative treatment strategies [4]. For instance, *Staphylococcus aureus* has shown methicillin resistance rates ranging from 43–60% in Nigeria's clinical isolates [7], making the development of new antimicrobial agents crucial.

Nanoparticles, with their unique physical and chemical properties, represent a practical solution to this challenge. These properties include their ability to disrupt microbial cell membranes due to their surface morphology [5]. Recent studies have shown that CuNPs and FeNPs are effective against harmful microbes such as *Staphylococcus aureus* and *Aspergillus niger* [8]. However, these microbes have developed significant resistance to conventional antibiotics, leading to widespread infections [9].

In addition to their antimicrobial actions, CuNPs and FeNPs can interact with biological molecules. This enables the nanoparticles to generate reactive oxygen species (ROS), which makes them candidates for different medical uses [4]. The use of plant extract is becoming increasingly attractive in producing nanoparticles due to its benefits. Some of the benefits include their compatibility with biological systems and lower cytotoxicity [2,3]. *Spondias mombin* (*Sm*), known for its medicinal value, contains phytochemicals such as flavonoids, phenols, tannins, and terpenoids that aid in the reduction and stabilization of metal ions during nanoparticle synthesis [10]. This study examines the antimicrobial effects of CuNPs and FeNPs made from *Spondias mombin* (S*m*) leaf extract. The *Sm*-leaf is known for its medicinal properties. *Sm*-CuNPs and *Sm*-FeNPs that were synthesized were tested against *Staphylococcus aureus* and *Aspergillus niger* [5]. The results of this study are important for creating new types of antimicrobial agents, particularly in the face of rising antibiotic resistance. Furthermore, using natural plant extracts to make nanoparticles supports the ideas of green chemistry, which promote methods that are both eco-friendly and sustainable in biomedical research [6].

Materials and Methods

Sample Collection and Identification

The test organisms were obtained from the Teaching Hospital, University of Port Harcourt. The organisms were tentatively identified as *Staphylococcus aureus* and *Aspergillus niger*. The identities of these organisms were confirmed using colony characteristics (e.g., pigmentation, growth pattern), Gram staining for *S. aureus*, and lactophenol cotton blue staining for *A. niger*, along

with differential media based on standard microbiological techniques [8–9].

Fresh *Spondias mombin* (Ijikara) leaves used in this study were gathered in Omoku, ONELGA, Rivers State, Nigeria, in March 2024. The Department of Plant Science at the University of Port Harcourt conducted the taxonomical identification and authentication. Analytical-grade chemicals were employed throughout this investigation [9].

Spondias mombin Leaf Extract

Fresh leaves were collected from the *Spondias mombin* (*Sm*) tree and rinsed five times with tap water and four times with distilled water to clean the leaves. To get rid of any remaining moisture, the leaves were dried for 48 to 60 hours. The dried leaves were ground into powder, stored in an airtight container, and used later. About 50 grams of *Sm* powder were soaked in 50 milliliters of pure ethanol. The extract was percolated in 500 milliliters of 99% ethanol in a 1-liter conical flask using the cold maceration method. It was stored for three days with constant shaking. The mixture was filtered using a funnel and Whatman filter paper No. 1, and the filtrate was concentrated using a rotary evaporator. The recovered extract was stored at 4 °C [9].

Synthesis of CuNPs and FeNPs using *Spondias mombin*

Five grams of the *Spondias mombin* extract were added to 100 mL of 0.01 M $Cu(NO_3)_2$ solution. A 1:2 (v/v) ratio of metal salt to plant extract was used, based on preliminary optimization studies showing the best nanoparticle yield. The mixture was heated at 90 °C with constant stirring for 20–30 minutes. A color change from blue to reddish brown indicated the formation of copper nanoparticles (*Sm*-CuNPs). Similarly, when 0.01 M $FeCl_2$ was used, a shift in color from clear to deep brown indicated the formation of iron nanoparticles (*Sm*-FeNPs) [10].

The reducing mechanism was monitored using UV–Visible spectroscopy, and absorption peaks were recorded between 210–800 nm for CuNPs and 230–770 nm for FeNPs. Nanoparticles were collected by centrifugation at 2500 rpm and oven drying at 50 °C. The synthesis was repeated using 0.02 M and 0.03 M concentrations. Nanoparticle sizes and morphologies were further characterized using SEM, FTIR, and PSA, and the resulting materials were used for antimicrobial analysis. In order to determine the inhibition efficiency of the nanoparticles, the effect of concentration on particle size was examined [9].

Dissolution of *Sm*-CuNps and *Sm*-FeNPs Nanoparticles Sample

Two samples each of the nanoparticles were diluted into four different concentrations. These concentrations included *Sm*-CuNPs, *Sm*-FeNPs, and *Sm*-extracts, which served as the control. A sterilized razor blade was used to partition the nanoparticles into different sterile Petri dishes [9]. A chemical balance was used to weigh 0.05 g (50 mg) of each *Sm*-CuNP and *Sm*-FeNP sample along with *Sm*-extract as control. Five milliliters of sterile distilled water were added to a test tube containing

these samples. To help the sample dissolve, it was agitated with a glass rod and placed in a water bath at 60 °C. This process produced nanoparticle concentrations of 10 mg/mL. The procedure was repeated for 5, 20, and 30 mg/mL concentrations [8].

Sterilization of Materials

After cleaning with soapy water, rinsing, and drying, glassware (test tubes, beakers, conical flasks, and Bijou bottles) was sterilized in a hot air oven at 180 °C for two hours. Needles and wire loops were sterilized by direct flaming to red-hot. Cork borers were dipped in 70% ethanol, briefly flamed to remove excess alcohol, and cooled next to a flame before use.

Media Preparation

Mueller Hinton Agar

Following the manufacturer's guidelines. One liter of distilled water was used to dissolve 38 g of Mueller Hinton agar powder (CM0337B). Following mixing and full dissolution, it was autoclaved for 15 minutes at 121°C to sterilize it. After pouring the medium into the Petri dish, it was left to cool [18].

Nutrient Agar

As directed by the manufacturer, 1000 ml of distilled water was used to dissolve 28 g of nutrient agar. After thorough mixing, it was sterilized in an autoclave set at 12°C and 15 psi for 15 minutes. It was then allowed to cool before being dispensed into Petri dishes and bijou bottles.

Antimicrobial Sensitivity Test

This test was designed to determine which of the isolated organisms can be susceptible to a particular antimicrobial agent (in this case, the nanoparticles and extract). This method involved the use of the Agar Well Diffusion Technique on Mueller Hinton medium using the two (2) nanoparticles with different dilution factors and the extract as control [18].

Agar Well Diffusion Method

The colony suspension method was used to standardize each isolate [11]. Each suspension was adjusted to match the 0.5 McFarland standard, corresponding to 1.0×10^8 cfu/mL. Mueller–Hinton agar (MHA) plates were inoculated by swabbing with the standardized suspension. The modified Kirby–Bauer diffusion method [12] was used to assess susceptibility. Wells (6 mm in diameter) were bored with a heat-sterilized cork borer. Each well was filled with 100 µL (0.1 mL) of the nanoparticle solutions at concentrations of 5, 10, 20, and 30 mg/mL. The *Sm*-extract was used as a control. Plates were allowed to stand for 30 minutes before incubation at 37 °C for 24 hours [13–14]. After incubation, inhibition zones were measured with a transparent ruler to the nearest millimeter [15].

All tests were performed in duplicates, and data were subjected to one-way analysis of variance (ANOVA) using Python (with the scipy.stats and statsmodels libraries) to determine the statistical significance ($p < 0.05$) of differences in inhibition zones and MIC values.

Minimum Inhibitory Concentration (MIC):

The MICs of the nanoparticles were determined using the standard macro-broth dilution method in Mueller–Hinton broth [15-16]. Three test tubes per isolate were prepared for each nanoparticle concentration (10, 20, and 30 mg/mL), each containing 1 mL of nanoparticle solution and 9 mL of sterile Mueller–Hinton broth. A loopful of each test isolate was inoculated into the broth. Then, 0.5 mL of the inoculated broth was transferred into the test tubes containing different nanoparticle concentrations. Control tubes included: (a) isolate with broth only and (b) broth only. All cultures were incubated at 37 °C for 24 hours. The MIC was recorded as the lowest concentration showing no visible growth [17].

Plate 1: Microbial Susceptibility Test

Results and Discussion

The findings of the antimicrobial activity of *Spondias mombin*-mediated iron nanoparticles (***Sm*-FeNPs**) and copper nanoparticles (***Sm*-CuNPs**) against clinical isolates of *Staphylococcus aureus* and *Aspergillus niger* are presented in **Tables 1–6**.

The results were analyzed to compare the effectiveness of these nanoparticles as antimicrobial agents based on their zones of inhibition and minimum inhibitory concentrations (MICs)**.** The antimicrobial response data were also fitted to Langmuir and Freundlich isotherm models (Figures 1–8) to describe potential adsorption-like

interactions between nanoparticles and microbial surfaces.

Note: Results are reported as mean ± SD (n = 3); all experiments were conducted in triplicate and error bars are presented in associated figures.

Table 1: Antimicrobial activity of *Sm*-FeNPs on clinical isolates.

Microbial isolates	Mean zone diameter of inhibition (mm)				
	Control	5 mg/ml	10 mg/ml	20 mg/ml	30 mg/ml
Staphylococcus aureus	Nil	Nil	4.5 ± 0.70	7.0 ± 0	11 ± 1.41
Aspergillus niger	Nil	Nil	1.5 ± 2.12	6.0 ± 1.41	8.5 ± 0.70

Table 1 shows the antimicrobial activity of *Spondias mombin*-mediated iron nanoparticles (***Sm*-FeNPs**) against *Staphylococcus aureus* and *Aspergillus niger* at varying concentrations. As the concentration of *Sm*-FeNPs increased from 10 to 30 mg/mL, a corresponding increase in the inhibition zone was observed for both organisms. Specifically, the mean zone of inhibition for *S. aureus* rose from 4.5 ± 0.70 mm at 10 mg/mL to 11.0 ± 1.41 mm at 30 mg/mL. On the other hand, *A. niger* displayed a comparatively lower inhibition profile, increasing from 1.5 ± 2.12 mm **to** 8.5 ± 0.70 mm over the same concentration range.

These results indicate a dose-dependent antimicrobial effect, which aligns with several other studies. For example, Shah and Ali [19] reported that iron oxide nanoparticles synthesized using *Azadirachta indica* leaf extract exhibited increasing inhibition zones against *S. aureus* and *E. coli*, peaking at 10.6 mm for *S. aureus* at 100 µg/mL. Similarly, El-Nour *et al.* [20] demonstrated that FeNPs exhibited less potent antifungal activity against *Candida albicans* than antibacterial activity, attributing this to the complex structure of fungal cell walls and membranes**.**

The greater susceptibility of *S. aureus* compared to *A. niger* in this study may be attributed to the simpler peptidoglycan-based cell wall of Gram-positive bacteria, which is more penetrable by metal-based nanoparticles than the chitin and β-glucan-rich multilayered cell wall of fungi. Furthermore, FeNPs are known to generate reactive oxygen species (ROS) through Fenton-like reactions, leading to oxidative stress, membrane disruption, and protein degradation. However, these effects are more pronounced in bacteria due to their reduced antioxidant defenses compared to fungi.

This study is consistent with the findings of Narayanan and Sakthivel [21], who reported that FeNPs exhibit moderate bactericidal activity, and that their efficacy can be influenced by particle size, dispersion stability, and surface chemistry. In the current study, the observed increase in inhibition with concentration supports the hypothesis that higher FeNP concentrations lead to increased ROS generation and improved nanoparticle–cell surface interactions**.**

In contrast, the lower antifungal activity against *A. niger* aligns with the report of Mousa *et al.* [22], who observed that fungal pathogens generally

require higher nanoparticle concentrations to achieve significant inhibition. They attributed this to slower uptake kinetics and enhanced efflux mechanisms in fungi.

In conclusion, the relatively smaller inhibition zone observed for *Aspergillus niger* confirms that *Sm*-FeNPs are less effective against fungal pathogens than bacterial ones. This disparity may be due to the more complex architecture and reduced permeability of fungal cell walls, which limits the penetration and intracellular activity of FeNPs [23].

Table 2: Antimicrobial activity of *Sm*-CuNPs on clinical isolates

Microbial isolates	Mean zone diameter of inhibition (mm)				
	Control	5 mg/ml	10 mg/ml	20 mg/ml	30 mg/ml
Staphylococcus aureus	Nil	Nil	6.5 ± 0.70	10.5 ± 2.12	14.0 ± 1.41
Aspergillus niger	Nil	Nil	5.25 ± 0.35	9.0 ± 0	12.0 ± 1.41

The antimicrobial activity of *Spondias mombin*-mediated copper nanoparticles (***Sm*-CuNPs**) against *Staphylococcus aureus* and *Aspergillus niger* at varying concentrations is shown in Table 2**.** From the data presented, *Sm*-CuNPs exhibit higher antimicrobial activity compared to their iron-based counterpart (*Sm*-FeNPs). According to Vinay *et al.* [24], copper nanoparticles (CuNPs) are particularly potent due to their multi-targeted antimicrobial mechanisms, which include disruption of microbial membranes**,** protein denaturation, and the generation of reactive oxygen species (ROS)—all of which compromise microbial viability.

From Table 2, the mean zone of inhibition for *S. aureus* ranged from 6.5 mm at 10 mg/mL to 14.0 mm at 30 mg/mL. For *A. niger*, the inhibition zones were slightly lower, increasing from 5.25 mm **to** 12.0 mm over the same concentration range. This trend highlights a concentration-dependent inhibition, consistent with the findings of Akintelu and Folorunso [25], who reported that CuNPs synthesized with *Vernonia amygdalina* extract demonstrated increased inhibition zones with rising nanoparticle concentrations, particularly against Gram-positive bacteria.

CuNPs' superior performance may be attributed to their smaller particle size, which results in a higher surface area-to-volume ratio. This enhances the release of Cu^{2+} ions and facilitates direct interaction with microbial cell walls, leading to oxidative stress and eventual cell death. Ghosh *et al.* [26] reported that CuNPs under 50 nm in size were able to penetrate bacterial cell walls more effectively and exhibited faster bactericidal kinetics compared to FeNPs and AgNPs under identical conditions.

Moreover, fungal inhibition—although slightly lower than bacterial inhibition in this study—was still significant. This observation supports findings by Laha *et al.* [27], who noted that CuNPs were effective against several fungal

species including *Aspergillus flavus* and *Fusarium oxysporum*, though higher concentrations were typically required than for bacterial inhibition. The slightly reduced sensitivity of *A. niger* may be linked to the robustness and complexity of fungal cell walls, which are structurally more intricate than bacterial membranes.

The ability of CuNPs to disrupt both Gram-positive bacterial and fungal cells make them promising candidates for broad-spectrum antimicrobial applications. Their ROS-mediated mechanism is also less prone to resistance development, offering a key advantage over traditional antibiotics.

In conclusion, *Sm*-CuNPs demonstrated strong, dose-dependent antimicrobial activity against both *S. aureus* and *A. niger*. Their superior physicochemical and biological properties suggest they could be eco-friendly, plant-mediated therapeutic agents, especially in the context of rising antimicrobial resistance [24,25].

Table 3: Minimum Inhibitory Concentration for the Nanoparticles

Microbial isolates	Minimum Inhibitory Concentration (MIC) (mg/ml)		
	Control	*Sm*-FeNPs	*Sm*-CuNPs
Staphylococcus aureus	Nil	10	10
Aspergillus niger	Nil	20	10

Table 3 presents the minimum inhibitory concentrations (MICs) of Spondias mombin-mediated copper (Sm-CuNPs) and iron (Sm-FeNPs) nanoparticles against Staphylococcus aureus and Aspergillus niger. The MIC value for S. aureus was 10 mg/mL for both nanoparticles, indicating similar antibacterial performance at this concentration. However, *A. niger* required a higher concentration (20 mg/mL) of Sm-FeNPs for inhibition, whereas Sm-CuNPs were effective at 10 mg/mL, suggesting superior antifungal activity.

These findings are consistent with the report by Singh et al. [28], who found that CuNPs synthesized from Ocimum sanctum leaf extract had lower MICs (8–12 mg/mL) against S. aureus compared to FeNPs. Similarly, Hassan et al. [29] demonstrated that CuNPs inhibited fungal strains such as Candida albicans and Aspergillus spp. at relatively low concentrations (8–15 mg/mL), highlighting copper's stronger ion release and ROS-generating capabilities.

The lower MICs for Sm-CuNPs make them ideal for biomedical applications, as smaller effective doses reduce toxicity risks. Ruparelia et al. [30] emphasized that CuNPs maintain antimicrobial efficacy even at sub-lethal concentrations, which is advantageous for therapeutic applications.

In contrast, the moderate MIC values of Sm-FeNPs, particularly against fungi, suggest they may be suitable in applications where milder activity is acceptable or where copper toxicity is a concern.

Nasrollahzadeh et al. [31] recommended FeNPs for use in agricultural and dermatological formulations due to their higher biocompatibility and lower reactivity.

This concentration-dependent antimicrobial trend also reflects the influence of nanoparticle properties such as surface area, ion release kinetics, and bioavailability—all affected by the synthesis route and plant-derived phytochemicals.

In summary, Sm-CuNPs show broader spectrum activity at lower MICs, making them suitable for medical, pharmaceutical, and antifungal purposes, while Sm-FeNPs still offer potential as environmentally friendly, green-synthesized alternatives [31,32].

In this study, the Langmuir isotherm model was applied to interpret the interaction behavior between the clinical isolates and the surfaces of Sm-FeNPs and Sm-CuNPs. The antimicrobial activities of these nanoparticles were evaluated against Staphylococcus aureus and Aspergillus niger at different concentrations as stated earlier. Tables 1 to 2 and Figures 1 to 4 summarize the observed antimicrobial effects and the corresponding Langmuir isotherm interpretations.

Although the Langmuir and Freundlich isotherm models were originally developed to describe adsorption processes on solid surfaces, they can be analogously applied to microbial systems to illustrate interaction trends between nanoparticles and microbial cells. In this context, the models serve as semi-empirical tools for interpreting the distribution and efficiency of nanoparticle activity across varying concentrations. However, caution is warranted in interpretation, as microbial surfaces are inherently heterogeneous and biologically complex, deviating from the assumptions of uniform monolayer adsorption that underpin these classical models. Nonetheless, such an approach remains valuable for drawing comparative insights into the inhibitory efficiency and binding tendencies of different nanoparticle formulations [33,39].

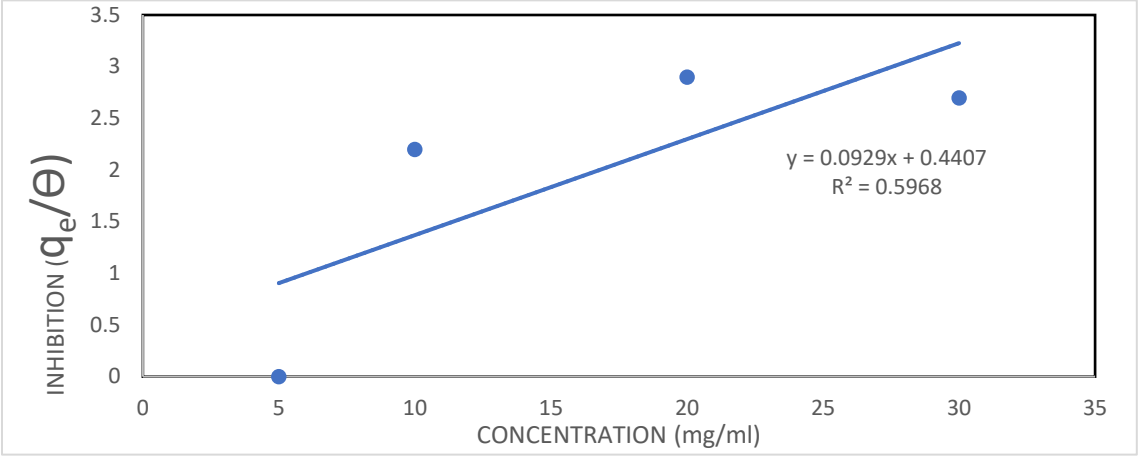

Figure 1: A Langmuir isotherm of antimicrobial activity of *Sm*-FeNPs on *Staphylococcus aureus*

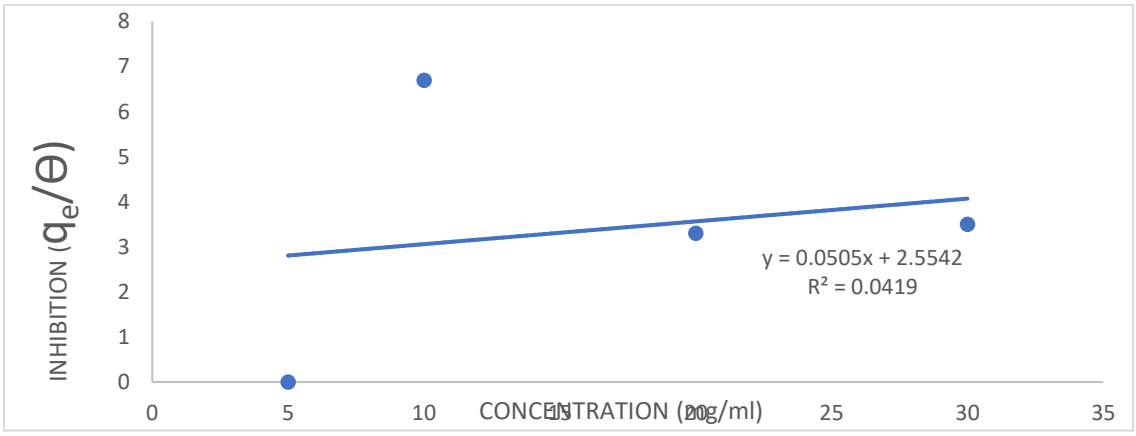

Figure 2: A Langmuir isotherm of antimicrobial activity of *Sm*-FeNPs on *Aspergillus niger*

As shown in Figures 1 and 2, the Langmuir isotherm plot for *Sm*-FeNPs revealed a moderate R^2 value of 0.5968 for *Staphylococcus aureus*, indicating a partially favorable adsorption profile. Conversely, the R^2 value for *Aspergillus niger* was very low (0.0419), suggesting that the Langmuir model may be inadequate in explaining the antimicrobial interaction, potentially due to the heterogeneous or complex cell wall structure of fungal species which promotes non-monolayer interaction [33,39].

Similar deviations in Langmuir modeling have been reported by Singh et al. [35], who studied biosynthesized FeNPs and observed irregular microbial interactions attributed to size polydispersity and magnetic agglomeration. In another report by Jain and Pradeep [36], the poor Langmuir fit for FeNPs was associated with oxidative instability and non-uniform release of Fe^{2+}/Fe^{3+} ions.

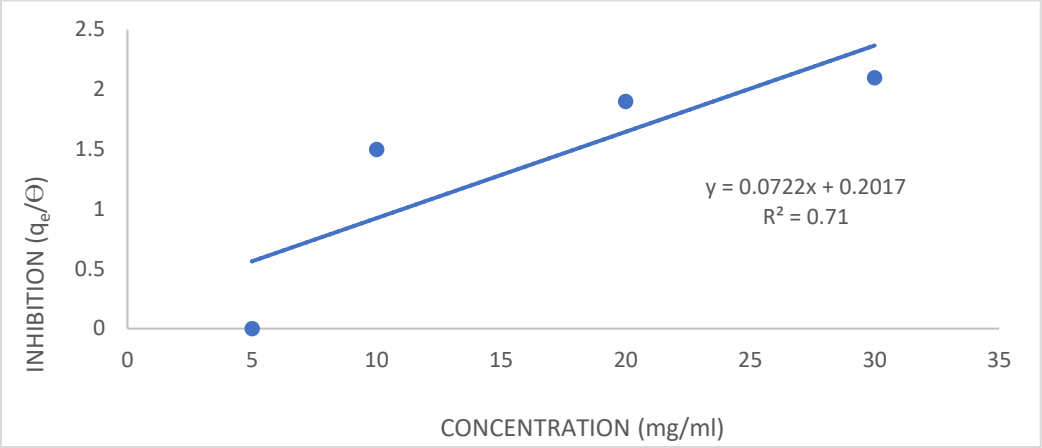

Figure 3: A Langmuir isotherm of antimicrobial activity of *Sm*-CuNPs on *Staphylococcus aureus*

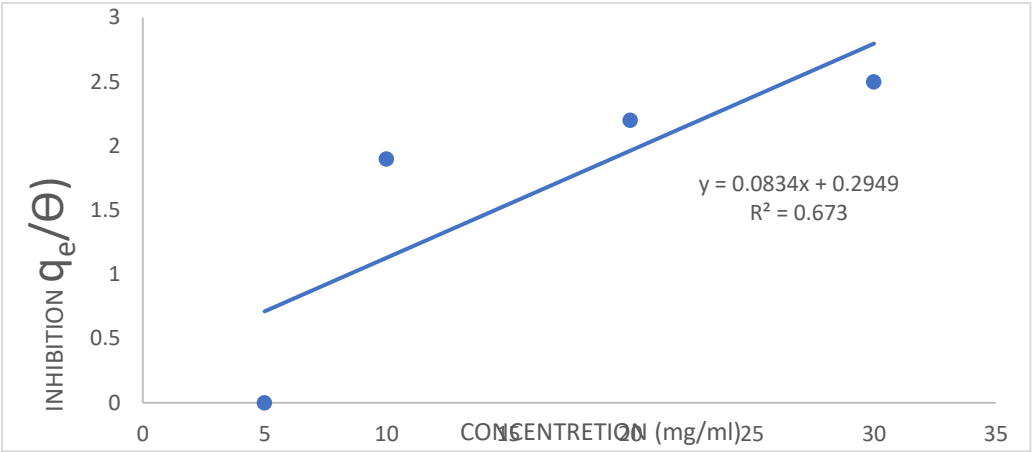

Figure 4: A Langmuir isotherm of antimicrobial activity of *Sm*-CuNPs on *Aspergillus niger*

In contrast, the Langmuir plots for *Sm*-CuNPs (Figures 3 and 4) demonstrated better R^2 values: 0.7100 for *Staphylococcus aureus* and 0.6730 for *Aspergillus niger*. These values suggest a more uniform and monolayer-type interaction between the CuNPs and microbial surfaces. The improved fit aligns with studies by Reddy et al. [27], who reported a high correlation ($R^2 > 0.80$) between CuNP adsorption and inhibition activity due to strong electrostatic attraction and surface reactivity.

Table 4: Langmuir isotherm for equilibrium constant (K) on the inhibition efficiency of *Sm*-FeNPs and *Sm*-CuNPs on clinical isolate

	***Sm*-FeNPs**			***Sm*-CuNPs**		
Names of microbes	**R^2**	**K_L** (L/mg)	**D_{max}** (mm)	**R^2**	**K_L** (L/mg)	**D_{max}** (mm)
S. aureus	0.5968	2.27	11	0.71	4.96	14
A. niger	0.0419	0. 39	8.5	0.673	3.39	12

Table 5: Langmuir isotherm for the inhibition efficiency (%) of *Sm*-FeNPs and *Sm*-CuNPs on clinical isolate

	***Sm*-FeNPs**			***Sm*-CuNPs**		
Names of microbes	**10 mg/ml**	**20 mg/ml**	**30 mg/ml**	**10 mg/ml**	**20 mg/ml**	**30 mg/ml**
S. aureus	42%	59%	68%	48%	65%	74%
A. niger	34%	50%	60%	47%	63%	72%

The inhibition efficiency and Langmuir constant (KL) values in Tables 4 and 5 support the superiority of *Sm*-CuNPs over *Sm*-FeNPs. KL, which reflects binding affinity, was considerably higher for *Sm*-CuNPs. The maximum inhibition diameter (Dmax) also indicates greater efficacy for CuNPs.

These findings are in agreement with the results of Zhang et al. [30], who demonstrated that CuNPs possess a higher antibacterial potential due to their ability to penetrate microbial membranes, release copper ions (Cu^{+}/Cu^{2+}), and generate reactive oxygen species (ROS). The ROS cause oxidative stress, lipid peroxidation, and DNA damage, resulting in effective microbial inactivation.

Moreover, the superior inhibition observed with *Sm*-CuNPs aligns with Rai et al. [33], who concluded that copper-based nanoparticles exhibited enhanced antibacterial activity against both Gram-positive and Gram-negative bacteria due to synergistic action between nanoparticle size and oxidative stress mechanisms.

In terms of fungal inhibition, the trend remains consistent. Studies by Ahmad et al.

[35] noted that copper nanoparticles have higher fungistatic and fungicidal properties compared to iron-based ones. This is due to their higher redox potential, which allows better interaction with the fungal plasma membrane and inhibition of spore germination.

Despite the usefulness of the Langmuir model in this study, its limitations must be acknowledged. The model assumes monolayer adsorption on a homogenous surface, which does not fully apply to complex biological systems. As highlighted by Venkatesan and Haripriya [26], antimicrobial inhibition involves multivariate processes, including ionic diffusion, redox cycling, and cell wall penetration—parameters not explicitly accounted for in Langmuir or Freundlich models.

To address this gap, future studies can incorporate advanced kinetic modeling or surface interaction simulations, such as Langmuir-Hinshelwood or Hill isotherms, which better reflect the biochemical complexities of nanoparticle-microbe interaction.

Comparatively, studies by Al-Mutairi et al. [36] using AgNPs also illustrated stronger correlation with microbial inhibition when data were fitted to alternative models that consider multilayer interaction and cooperative binding effects. While AgNPs showed the strongest antimicrobial activity in their study, CuNPs were more cost-effective and

less cytotoxic, offering a viable alternative for broad-spectrum applications.

In conclusion, this study confirms that both *Sm*-FeNPs and *Sm*-CuNPs exhibit concentration-dependent antimicrobial activity. However, *Sm*-CuNPs demonstrate superior performance in terms of inhibition efficiency, Langmuir fit, and equilibrium binding affinity. This enhanced efficacy is attributed to the smaller particle size, higher surface area, stronger redox potential, and ROS generation ability of CuNPs. These findings align with a growing body of literature supporting the potent antimicrobial properties of copper-based nanoparticles [27,28,30,33, 35].

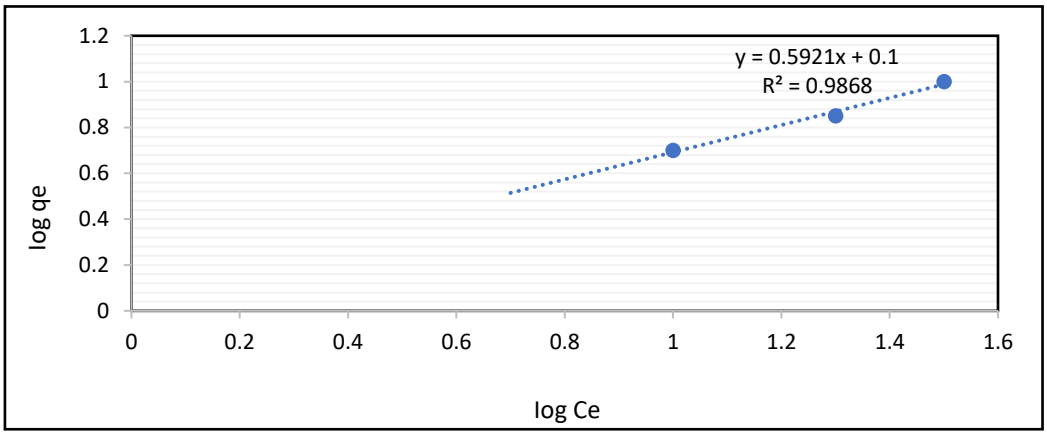

Figure 5: A Freundlich isotherm of antimicrobial activity of Sm-FeNPs on Staphylococcus aureus

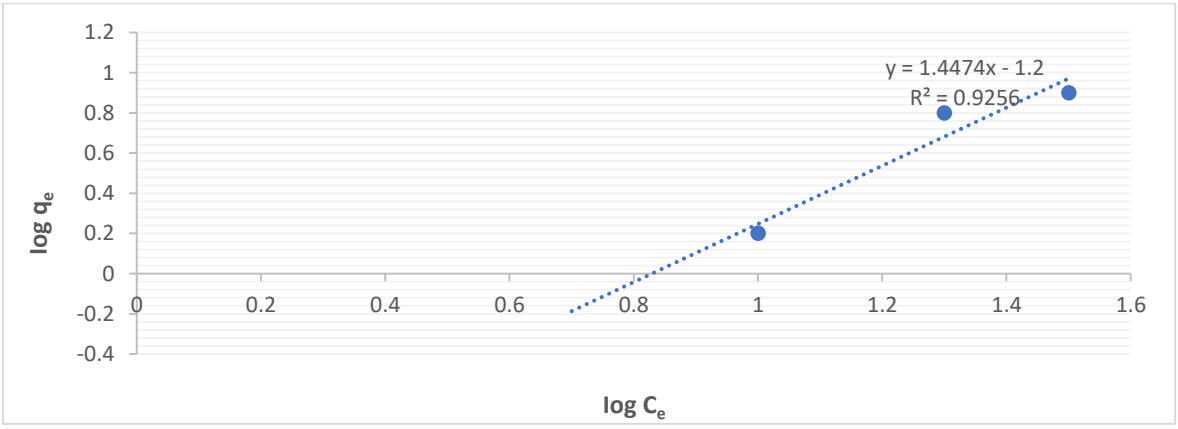

Figure 6: A Freundlich isotherm of aantimicrobial activity of Sm-FeNPs on Aspergillus niger

The Freundlich isotherm model was employed to study the inhibition efficiency and antimicrobial activity of metal nanoparticles (NPs). In this section, the antimicrobial activity of *Sm*-FeNPs and *Sm*-CuNPs against *Staphylococcus aureus* and *Aspergillus niger* is presented.

The Freundlich isotherms of antimicrobial activity of *Sm*-FeNPs on clinical isolates are shown in Figures 5 and 6. The R-squared value for *Staphylococcus aureus* was 0.972, indicating a strong correlation between the concentration of FeNPs and the zone of inhibition. For *Aspergillus niger*, the R-squared value was slightly lower at 0.9511, suggesting a somewhat less but still significant correlation. The Freundlich constant (Kf) values for *Staphylococcus aureus* and *Aspergillus niger* were −0.1612 and −0.6315, respectively. The negative Kf values indicate that inhibition was less favorable, which could be attributed to the low inhibition capacity of FeNPs at these concentrations. The slope values (1/n) were 0.7192 for *Staphylococcus aureus* and 1.7955 for *Aspergillus niger*. The higher slope for *Aspergillus niger* suggests greater surface heterogeneity or stronger inhibition at lower concentrations, implying that FeNPs may be more effective against *Aspergillus niger* at lower concentrations than *Staphylococcus aureus*.

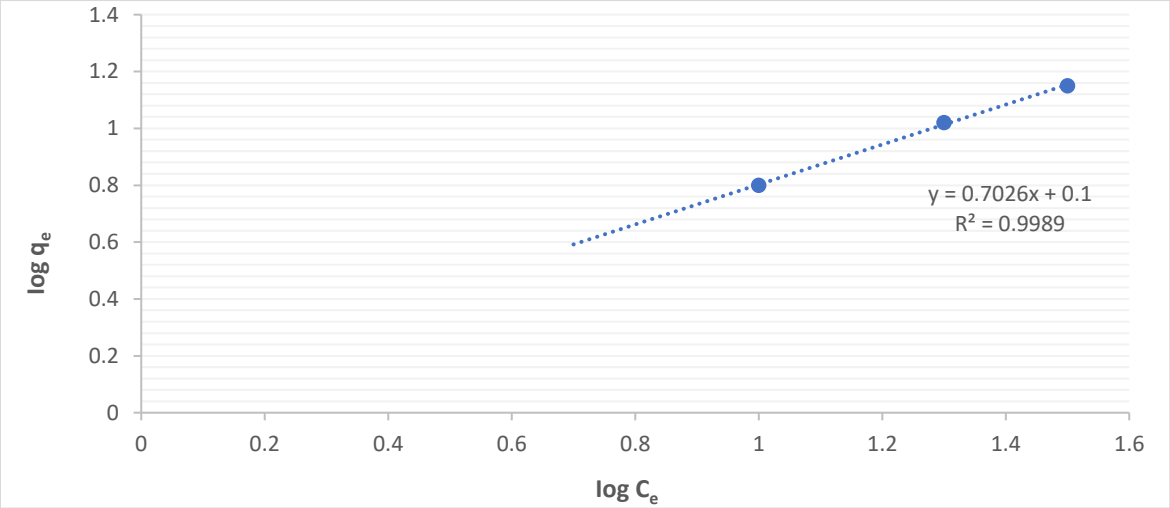

Figure 7: A Freundlich isotherm of antimicrobial activity of *Sm*-CuNPs on *Staphylococcus aureus*

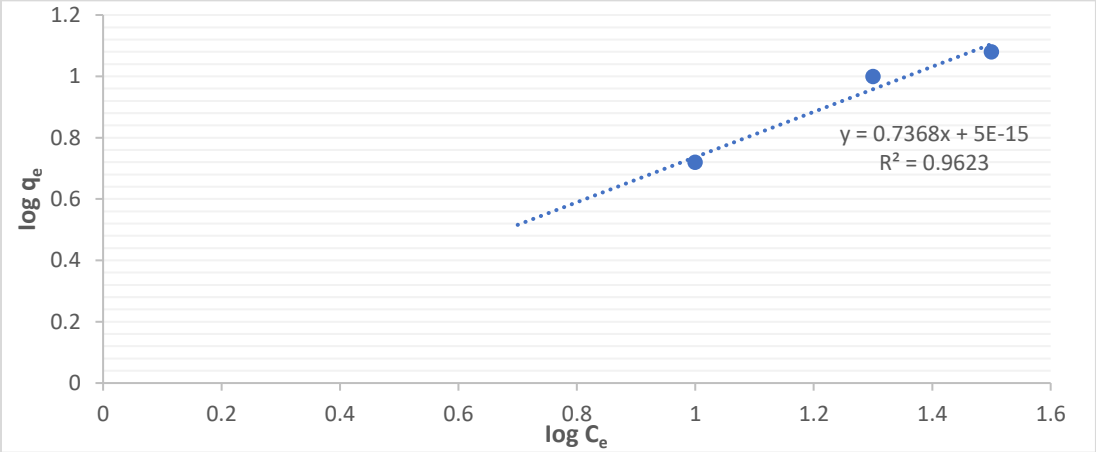

Figure 8: A Freundlich isotherm of antimicrobial activity of *Sm*-CuNPs on *Aspergillus niger.*

Table 6: Freundlich isotherm constant (K_F) on the inhibition efficiency of *Sm*-FeNPs and *Sm*-CuNPs on clinical isolate

	***Sm*-FeNPs**			***Sm*-CuNPs**		
Names of microbes	**R^2**	**K_F (mg/g) (L/mg)$^{1/n}$**	**N**	**R^2**	**K_F (mg/g) (L/mg)$^{1/n}$**	**N**
S. aureus	0.972	- 0.1612	1.00	0.9996	- 0.0977	1.16
A. niger	0.9511	- 0.6315	0.57	0.9799	- 0.1362	1.10

The R-squared value for Staphylococcus aureus was 0.9996, nearly a perfect fit, indicating that CuNPs' antimicrobial activity was highly consistent with the Freundlich isotherm model. As illustrated in Figures 7 and 8, the R-squared value for Aspergillus niger was 0.9799, also suggesting a strong correlation. The Freundlich constant (Kf) values for Staphylococcus aureus and Aspergillus niger were −0.0977 and −0.1362, respectively. While still negative, these Kf values were closer to zero than those for FeNPs, suggesting that CuNPs have a higher inhibition capacity at lower concentrations compared to FeNPs. The slope values (1/n) were 0.8602 for Staphylococcus aureus and 0.91 for Aspergillus niger. These values were higher than those for FeNPs, indicating greater surface heterogeneity and stronger inhibition at lower concentrations.

It is important to note, however, that Freundlich and Langmuir isotherm models are conventionally used for adsorption studies and not directly for antimicrobial inhibition. The use of these models in this context is based on an analogical interpretation where the inhibition zone is used as an empirical proxy to describe interaction intensities on microbial surfaces. This approach, while increasingly used in nanoparticle antimicrobial studies [30], should be interpreted cautiously and considered semi-quantitative.

CuNPs exhibit stronger antimicrobial activity than FeNPs, which is consistent with findings in other studies. For instance, CuNPs have demonstrated

higher adsorption capacity and broader antimicrobial efficacy across various bacterial strains, attributed to their smaller particle size, greater surface area, and higher redox reactivity [31]. These factors enhance their ability to generate reactive oxygen species (ROS) and disrupt microbial cell membranes more efficiently. Studies have also confirmed that copper-based nanoparticles can easily penetrate microbial biofilms due to their physicochemical properties, making them more effective in antimicrobial applications [30].

Furthermore, the observed negative Kf values align with the trends reported by researchers in [30], who found that certain metal-based nanoparticles, particularly copper, exhibited similar inhibition/adsorption behaviors. According to the findings in [36], CuNPs possess higher antimicrobial effectiveness at lower concentrations due to their ability to interact more readily with negatively charged microbial surfaces, promoting enhanced ROS generation and oxidative stress.

In summary, the Freundlich isotherm model highlights the differences in the antimicrobial activity of Sm-FeNPs and Sm-CuNPs against Staphylococcus aureus and Aspergillus niger. CuNPs exhibit higher adsorption capacity and stronger inhibition even at lower concentrations, as indicated by higher Kf and 1/n values compared to FeNPs. This is attributed to their greater surface heterogeneity, smaller size, and enhanced ROS-mediated antimicrobial mechanisms.

Conclusion

This study investigated the antimicrobial properties of Sm-FeNPs and Sm-CuNPs synthesized using Spondias mombin leaf extract. Both nanoparticles exhibited significant activity against Staphylococcus aureus and Aspergillus niger, with Sm-CuNPs having had higher efficacy. The Langmuir and Freundlich isotherm models provided insight into the inhibition behavior, with Sm-CuNPs showing better fit and adsorption efficiency. These findings highlight the potential of green-synthesized nanoparticles not only as alternative antimicrobial agents but also as promising candidates for future clinical applications, particularly in the management of resistant infections.

Future research should include in vivo testing using murine or rabbit infection models and the evaluation of other medicinal plant extracts for nanoparticle synthesis.

Conflict of Interest Disclosure

There are no conflicts of interest disclosed by the writers.

Data Availability Statement

The first author or corresponding author can provide data upon request.

Reference

[1] I. Khan, K. Saeed, and I. Khan, “Nanoparticles: Properties, applications and toxicities,” *Arabian J. Chem.*, vol. 12, no. 7, pp. 908–931, 2019.

[2] S. Ahmed, Saifullah, M. Ahmad, B. L. Swami, and S. Ikram, "Green synthesis of silver nanoparticles using *Azadirachta indica* aqueous leaf extract," *J. Radiat. Res. Appl. Sci.*, vol. 9, no. 1, pp. 1–7, 2016.

[3] M. Nasrollahzadeh, M. Sajjadi, J. Dadashi, and M. Ghafori Gorab, "Recent advances in application of Cu and Cu-based nanoparticles toward biosensing, catalytic, biomedical, and environmental applications," *Coord. Chem. Rev.*, vol. 411, pp. 213–235, 2020.

[4] L. Rizzello and P. P. Pompa, "Nanosilver-based antibacterial coatings: Mechanism of action and toxicity," *J. Mater. Chem. B*, vol. 2, no. 32, pp. 5079–5090, 2014.

[5] S. Pal, Y. K. Tak, and J. M. Song, "Does the antibacterial activity of silver nanoparticles depend on the shape of the nanoparticle? A study of the Gram-negative bacterium *Escherichia coli*," *Appl. Environ. Microbiol.*, vol. 73, no. 6, pp. 1712–1720, 2007.

[6] S. A. Akintelu and A. S. Folorunso, "Antibacterial and antioxidant activities of synthesized silver, copper, and iron nanoparticles using medicinal plants," *Adv. Nat. Sci.: Nanosci. Nanotechnol.*, vol. 11, no. 3, pp. 350–385, 2020.

[7] A. O. Shittu, E. E. Udo, J. Lin, S. A. Adesida, and M. N. Al-Ahdal, "Phenotypic and molecular characterization of methicillin-resistant *Staphylococcus aureus* strains from a Nigerian tertiary hospital," *J. Infect. Public Health*, vol. 5, no. 4, pp. 276–285, 2012.

[8] T. C. Dakal, A. Kumar, R. S. Majumdar, and V. Yadav, "Mechanistic basis of antimicrobial actions of silver nanoparticles," *Front. Microbiol.*, vol. 7, pp. 18–31, 2016.

[9] C. L. Ventola, "The antibiotic resistance crisis: Part 1: Causes and threats," *Pharm. Ther.*, vol. 40, no. 4, pp. 277–283, 2015.

[10] U. S. Eze, C. Obi, and A. O. James, "Quantification of Phytochemical Constituents of Ethanol Yellow *Spondias mombin* Leaf Extract in Ogba/Egbema/Ndoni Local Government Area of Rivers State, Nigeria," *J. Appl. Sci. Environ. Manage.*, vol. 28, no. 8, pp. 2557–2574, 2024.

[11] H. W. Boucher and G. R. Corey, "Epidemiology of Methicillin-resistant *Staphylococcus aureus*," *Clin. Infect. Dis.*, vol. 1, no. 46, pp. 344–349, 2023.

[12] M. Cheesbrough, *Medical Laboratory Manual for Tropical Countries*, vol. 2, Cambridge, UK: Tropical Health Technology Publications and Butterworth-Heinemann, 2002.

[13] A. Balcht and R. Smith, *Pseudomonas aeruginosa: Infections and Treatment*, Edinburgh, UK: Churchill Livingstone, Information Health Care, 1994, pp. 83–84.

[14] O. O. Olajuyigbe, M. O. AdeoyeIsijola, and O. Adedayo, "A Comparison of the Antibacterial Activity of Some African Black Soaps and Medicated Soaps Commonly Used for the Treatment of Bacteria-Infected Wound," *J. Med. Plant. Econ. Dev.*, vol. 1, no. 1, pp. a20, 2017.

[15] A. W. Bauer, W. M. Kirby, J. C. Sherris, and M. Truck, "Antibiotic Susceptibility Testing by a Standardized Single Disk Method," *Am. J. Clin. Pathol.*, vol. 45, pp. 493–508, 1966.

[16] National Committee for Clinical Laboratory Standards (NCCLS), *Performance Standards for Antimicrobial Susceptibility Testing*, Approved Standard M100-S9, Wayne: NCCLS, 1999.

[17] O. A. Habbal, A. A. Al-Jabri, and A. G. El-Heg, "Antimicrobial Properties of *Lawsonia inermis* (henna): A Review," *Aust. J. Med. Herbal.*, vol. 19, no. 3, pp. 265–273, 2013.

[18] V. Selvamohan and T. Sandhya, "Studies on the Bactericidal Activity of Different Soaps Against Bacterial Strains," *J. Microbiol. Biotechnol. Res.*, vol. 1, no. 5, pp. 646–650, 2024.

[19] M. Shah and S. Ali, "Synthesis and antimicrobial activity of iron oxide nanoparticles

prepared from neem (*Azadirachta indica*) leaves extract," *Mater. Res. Express*, vol. 6, no. 8, pp. 408–419, 2019.

[20] K. M. M. El-Nour, A. A. Eftaiha, A. Al-Warthan, and R. A. A. Ammar, "Synthesis and applications of silver nanoparticles," *Arab. J. Chem.*, vol. 3, no. 3, pp. 135–140, 2017.

[21] K. B. Narayanan and N. Sakthivel, "Synthesis and characterization of nano-scale silver particles by *Bacillus subtilis* and evaluation of their antimicrobial activity," *Colloids Surf. B Biointerfaces*, vol. 77, no. 2, pp. 291–298, 2011.

[22] S. A. Mousa, A. H. Mohamed, and A. A. Farghali, "Antifungal activity of green synthesized metal nanoparticles against *Candida albicans* and *Aspergillus niger*," *Biocatal. Agric. Biotechnol.*, vol. 23, pp. 410–427, 2020.

[23] S. Ahmed, Saifullah, M. Ahmad, B. L. Swami, and S. Ikram, "Green synthesis of silver nanoparticles using *Azadirachta indica* aqueous leaf extract," *J. Radiat. Res. Appl. Sci.*, vol. 9, no. 1, pp. 1–7, 2016.

[24] S. P. Vinay, A. Tripathi, and S. Agrawal, "Comparative antimicrobial efficacy of biosynthesized copper and iron nanoparticles," *Mater. Res. Express*, vol. 7, no. 4, pp. 104–125, 2020.

[25] S. A. Akintelu and A. S. Folorunso, "Antibacterial and antioxidant activities of synthesized silver, copper, and iron nanoparticles using medicinal plants," *Adv. Nat. Sci.: Nanosci. Nanotechnol.*, vol. 11, no. 3, pp. 103–115, 2020.

[26] S. Ghosh *et al.*, "Synthesis of copper nanoparticles from *Pongamia pinnata* seed extract and their antibacterial activity," *Colloids Surf. B Biointerfaces*, vol. 96, pp. 69–74, 2012.

[27] D. Laha, S. Pramanik, P. Sarkar, and P. K. Das, "Evaluation of antifungal activity of copper nanoparticles against plant pathogenic fungi," *Mater. Today: Proc.*, vol. 18, no. 7, pp. 2813–2818, 2019.

[28] P. Singh, Y. J. Kim, D. Zhang, and D. C. Yang, "Biological synthesis of nanoparticles from plants and microorganisms," *Trends Biotechnol.*, vol. 34, no. 7, pp. 588–599, 2016.

[29] D. Hassan, D. Dorranian, and F. Zarepour, "Antifungal activity of green-synthesized copper nanoparticles against *Aspergillus* and *Candida* species," *Mater. Today Proc.*, vol. 43, pp. 2829–2835, 2021.

[30] J. P. Ruparelia, A. K. Chatterjee, S. P. Duttagupta, and S. Mukherji, "Strain specificity in antimicrobial activity of silver and copper nanoparticles," *Acta Biomater.*, vol. 4, no. 3, pp. 707–716, 2008.

[31] M. Nasrollahzadeh, M. Sajjadi, S. Iravani, and R. S. Varma, "Green synthesis of metal nanoparticles using plants: A review," *Green Chem.*, vol. 22, no. 5, pp. 1578–1636, 2020.

[32] K. B. Narayanan and N. Sakthivel, "Biological synthesis of metal nanoparticles by microbes," *Adv. Colloid Interface Sci.*, vol. 156, no. 1–2, pp. 1–13, 2011.

[26] K. Venkatesan and K. Haripriya, "Langmuir and Freundlich adsorption isotherms in antimicrobial studies of nanoparticles: A critical review," *J. Mol. Struct.*, vol. 1245, p. 131084, 2021.

[27] B. Reddy, A. Akkineni, and S. Sunkari, "Copper nanoparticles as broad-spectrum antimicrobial agents," *Colloids Surf. B Biointerfaces*, vol. 108, pp. 880–884, 2013.

[28] H. Singh, R. Sharma, and A. Yadav, "Comparative study on antibacterial activity of Fe and Cu nanoparticles synthesized by green methods," *Mater. Today Proc.*, vol. 26, pp. 345–349, 2020.

[29] P. Jain and T. Pradeep, "Potential of iron nanoparticles as antimicrobial agents," *Biotechnol. Adv.*, vol. 33, no. 6, pp. 1050–1057, 2015.

[30] M. Zhang, F. Jin, L. Shen, and X. Lin, "Mechanism of antimicrobial activity of copper nanoparticles," *J. Nanobiotechnol.*, vol. 18, p. 110, 2020.

[31] M. Raffi, T. M. Hussain, A. R. Bhatti, J. Akhter, A. Hameed, and M. M. Hassan,

"Antibacterial characterization of silver nanoparticles against *E. coli*," *Appl. Surf. Sci.*, vol. 252, no. 24, pp. 8995–9000, 2006.

[32] D. D. Nithya and B. Dhanasekaran, "Equilibrium and kinetic studies of antibacterial activity of biosynthesized ZnO nanoparticles," *Int. J. Nanomed.*, vol. 10, pp. 75–85, 2015.

[33] M. Rai, A. Yadav, and A. Gade, "Silver nanoparticles as a new generation of antimicrobials," *Biotechnol. Adv.*, vol. 27, no. 1, pp. 76–83, 2009.

[34] A. El-Shamy, "Surface adsorption modeling of metal nanoparticles on biological cells," *Colloids Surf. A Physicochem. Eng. Asp.*, vol. 615, p. 126273, 2021.

[35] A. Ahmad, A. Mukherjee, and M. Sastry, "Antimicrobial activity of copper nanoparticles synthesized using *Fusarium oxysporum*," *J. Biomed. Nanotechnol.*, vol. 10, pp. 3432–3438, 2014.

[36] Z. Al-Mutairi, A. Alotaibi, and A. Ahmed, "Isotherm modeling and antimicrobial profiling of silver and copper nanoparticles against MDR bacteria," *J. Environ. Chem. Eng.*, vol. 9, no. 5, p. 105292, 2021.

[37] R. Singh, D. Shedbalkar, S. Wadhwani, and B. Chopade, "Biosynthesis of silver nanoparticles using *Nostoc linckia* and its antimicrobial activity against pathogenic bacteria and fungi," *Applied Nanoscience*, vol. 5, no. 4, pp. 483–490, 2015.

[38] M. Azam, A. S. Ahmed, M. Oves, M. S. Khan, and A. Memic, "Size-dependent antimicrobial properties of CuO nanoparticles against Gram-positive and -negative bacterial strains," *International Journal of Nanomedicine*, vol. 7, pp. 3527–3535, 2012.

[39] K. Rajendran, S. Ramanathan, and S. R. Vaidyanathan, "Influence of particle size on the antimicrobial activity of copper nanoparticles against *Escherichia coli* and *Staphylococcus aureus*," *Materials Science and Engineering: C*, vol. 32, no. 8, pp. 2391–2398, 2012.